

# Chiral Polyurethane Synthesis Leading to $\pi$ -Stacked 2/1-Helical Polymer and Cyclic Compounds

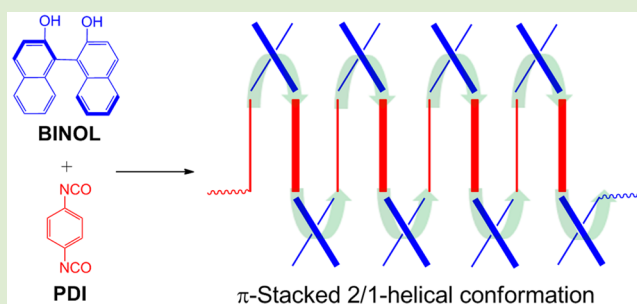
Prashant G. Gudeangadi,<sup>†</sup> Takeshi Sakamoto,<sup>†</sup> Yukatsu Shichibu,<sup>‡</sup> Katsuaki Konishi,<sup>‡</sup> and Tamaki Nakano<sup>\*,†</sup>

<sup>†</sup>Catalysis Research Center (CRC) and Graduate School of Chemical Sciences and Engineering, Hokkaido University, N21, W10, Kita-ku, Sapporo 001-0021, Japan

<sup>‡</sup>Faculty of Environmental Earth Sciences, Hokkaido University, N10, W5, Kita-ku, Sapporo 060-0810, Japan

## S Supporting Information

**ABSTRACT:** (*R*)-1,1'-Bi(2-naphthol) was reacted with 1,4-phenylene diisocyanate leading to a mixture of linear polyurethane and cyclic compounds including a cyclic dimer and a cyclic trimer. The structure of the cyclic dimer was elucidated by X-ray crystal structure analysis. The polymer was proposed to possess a rather stiff,  $\pi$ -stacked, 2/1-helical conformation on the basis of NMR, CD, and UV spectra and molecular dynamics simulations. The conformation was stable in the range of temperature of 0–60 °C.



Urethane bond is readily formed through a reaction between alcohol and isocyanate even without a catalyst, and a reaction between diol and diisocyanate leads to polyurethane. Polyurethane is an important class of polymer which can be applied for a wide variety of chemical products, including various types of foams, elastomers, fibers, coatings, and adhesives.<sup>1</sup> Further, aiming at more advanced functions, chiral polyurethanes have been prepared<sup>2</sup> since chirality plays an important role in attaining useful polymer properties.<sup>3</sup>

Herein we report the synthesis of a chiral polyurethane from optically active (*R*)-1,1'-bi(2-naphthol) (*R*-BINOL) and 1,4-phenylene diisocyanate (PDI). Binaphthyl is one of the most effective chiral organic groups in inducing a specific structure to a polymer, and a series of binaphthyl-based polymers were prepared and found to exhibit various functions, such as catalysis and light emission.<sup>4</sup> Although a BINOL-PDI reaction product was once reported,<sup>5</sup> its structure and reaction details have never been examined. This work focuses on the two aspects of the synthesis, that is, (i) chain topology (cyclic or linear) and (ii) chain conformation. As for chain topology, in general, a cyclic chain can form in addition to a linear chain in polyaddition or polycondensation. Formation of cyclic compounds has been explored for polyamides<sup>6</sup> and polylactones,<sup>7</sup> but not for a chiral polyurethane system. We found that both cyclic and linear chains are produced where their ratio can be controlled by tuning reaction conditions. As for chain conformation, a  $\pi$ -stacked, 2/1-helical conformation is proposed for the linear polymer. Such a conformation has been known only for limited polymers, including syndiotactic polystyrene and poly(*p*-methylstyrene) and some polydienes in the solid state.<sup>8</sup>

Reactions between *R*-BINOL and PDI were conducted in tetrahydrofuran (THF) in the presence of triethylamine (TEA) at a reagent concentration, [BINOL] = [PDI] = 0.031, 0.154, or 0.931 M and [TEA] = 0.48 M, at a temperature of 0, 23, or 60 °C for reaction durations from 5 s to 24 h (Scheme 1). The reactions were terminated by adding MeOH or by exposure to air. In all reactions examined in this study except for those for 3 min or shorter time, the monomers were almost completely consumed. The reaction products were found to include linear poly(BINOL-PDI), as well as oligomeric species, such as 1–3, indicated in Scheme 1.

Figure 1 shows the SEC curves of the polymerization products obtained by changing reagent concentration (A), temperature (B), and reaction time (C). In Figure 1A, the products obtained at 23 °C for 24 h at different monomer concentrations indicated noticeable, sharp peaks at around 19.5 min; the corresponding component was isolated by preparative SEC from the product obtained at [BINOL] = [PDI] = 0.154 M (Figure 1A (ii)), recrystallized from an ethyl acetate solution, and found to be a cyclic dimer (**1**) by X-ray crystallography (Figures 2 and S24 in the Supporting Information (SI)) and <sup>1</sup>H NMR spectrum (Figure 3A). The crystal of **1** contained ethyl acetate molecules that were also observed in the NMR spectrum. The NMR spectrum of **1** indicated a singlet signal of the -C<sub>6</sub>H<sub>4</sub>- group, indicating that **1** has rather high symmetry.

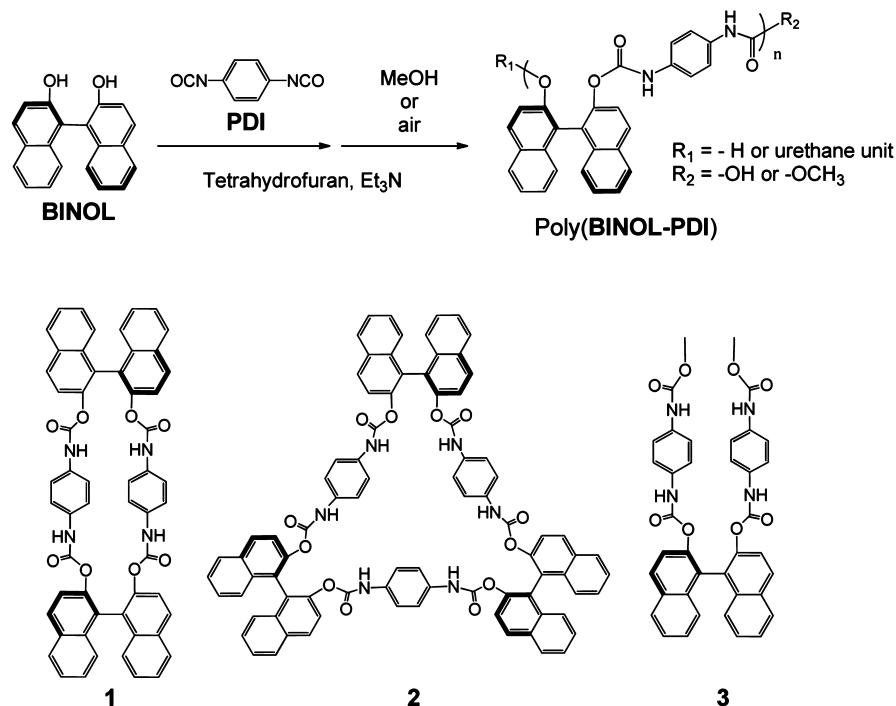
The component corresponding to the signal at 18.8 min was also isolated by preparative SEC from the product shown in Figure 1A (ii); this component indicated a mass number of

Received: July 12, 2015

Accepted: August 10, 2015

Published: August 12, 2015

Scheme 1. Polyaddition Reaction of BINOL with PDI Leading to a Polymer and Related Compounds



1361 corresponding to a cyclic trimer (**2**; exact mass: 1338.38) ion associated with sodium. In the  $^1\text{H}$  NMR spectrum of **2**, the signal of the  $-\text{C}_6\text{H}_4-$  group is not singlet, which is in line with the fact that **2** has lower symmetry compared with **1** (Figure 3B).

In Figure 1A, the dimer content varied depending on concentration and was estimated to be 55, 54, and 27% by peak area at  $[\text{BINOL}] = [\text{PDI}] = 0.031$  (iii), 0.154 (ii), and 0.931 M (i), respectively. At 0.931 M, a broad signal which may correspond to longer polymer chains was observed, indicating that the cyclic dimer formation is preferred at a lower concentration.

The molar mass distribution indicated in Figure 1A (i) is not normal, consisting of the polymer signal centered at 16.8 min and the oligomer mixture signals with the cyclic dimer as the highest one at 19.5 min. These results suggest that the polymer and oligomers may be formed through distinctive mechanisms.

A polymer sample ( $M_n = 6240$ ,  $M_w/M_n = 1.19$ , determined by SEC with right-angle light scattering detection) isolated by preparative SEC from the product in Figure 1A (i) indicated mass numbers corresponding to polymer chains having a terminal  $-\text{NCO}$  group in MALDI-mass spectra (SI, Figure S15). Further, a polymer prepared under the same conditions as those for Figure 1A (i) and terminated using MeOH indicated mass numbers corresponding to chains having both  $-\text{NCO}$  and  $-\text{NHCOOCH}_3$  groups at terminal (SI, Figure S16). These results indicate that the polymer samples contain linear chains, although a macrocyclic structure cannot be completely ruled out only with the given information.

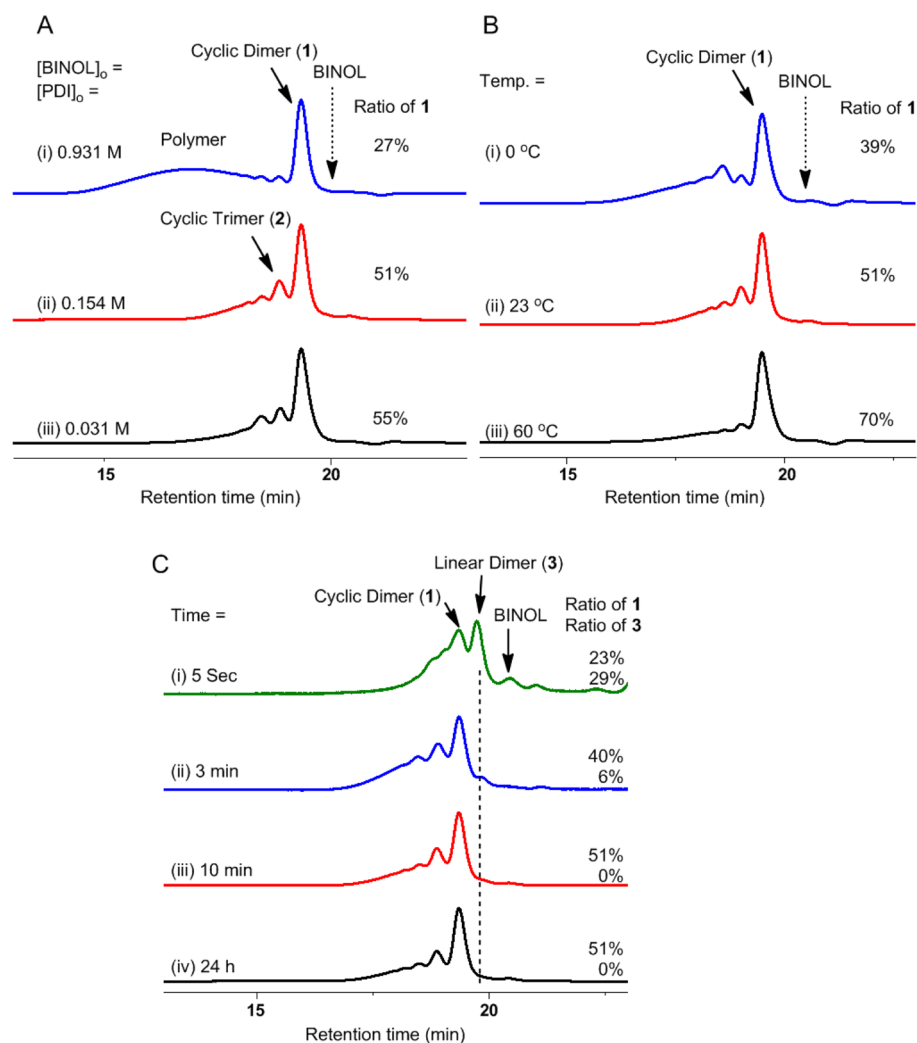
The results shown in Figure 1B where the reaction temperature varied at  $[\text{BINOL}] = [\text{PDI}] = 0.154$  M indicate that a higher temperature is suited to produce the cyclic dimer. On the basis of the effects of temperature and monomer concentration described so far, two extreme conditions were tested, namely, a reaction at 60 °C at  $[\text{BINOL}] = [\text{PDI}] = 0.031$  M aiming at the cyclic dimer, and that at 0 °C at

$[\text{BINOL}] = [\text{PDI}] = 0.93$  M aiming at polymer; the former led to 76% of the cyclic dimer and the latter to 75% of polymer (SI, Figures S20 and S21).

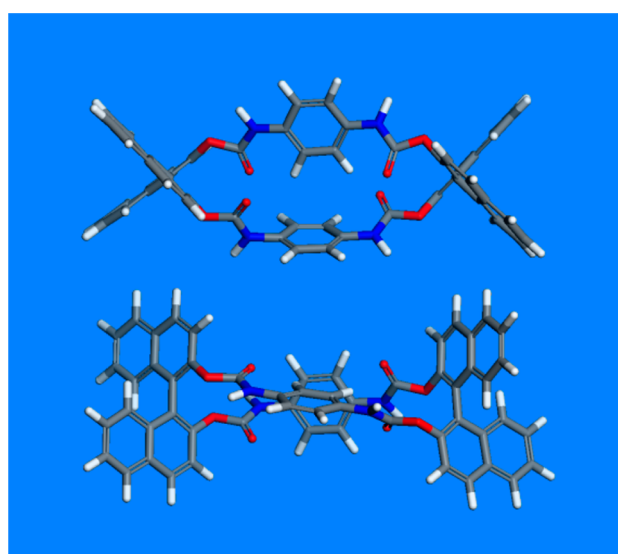
Further, time course of reaction was monitored in the range from 5 s to 24 h at  $[\text{BINOL}] = [\text{PDI}] = 0.154$  M at 23 °C (Figure 1C). BINOL was completely consumed and changes in SEC profiles ended within 10 min. In the SEC curve at 5 s, 16% of BINOL is still remaining, and a component is observed between the cyclic dimer and BINOL. This fraction isolated by preparative SEC showed a mass number of 693 (MALDI-mass spectrum) corresponding to a linear dimer (**3**; exact mass: 670.2064) ion associated with sodium. The  $^1\text{H}$  NMR spectrum of **3** indicated a clear  $-\text{OCH}_3$  signal at 3.71 ppm supporting the linear structure (Figure 3C). Compound **3** is clearly observed only in the 5 s reaction, suggesting that BINOL reacts first with two PDI molecules, independently or simultaneously, to form a diisocyanate compound corresponding to **3**, and the diisocyanate rapidly reacts with BINOL to form **1** or to grow to a longer, linear chain. Through such a mechanism, **1** and a linear polymer could have similar conformations stemmed from the same diisocyanate corresponding to **3**, where the BINOL moiety makes the main chain switch its direction.

Figure 3 compares the  $^1\text{H}$  NMR spectra of **1**, **2**, **3**, and the polymer. The polymer spectrum indicated far broader signals of the main chain compared with those of **1**–**3**, suggesting that the polymer has a very rigid conformation. In addition, the spectrum of the polymer exhibited upfield shifted aromatic signals in the range of 5.5–7 ppm, which indicates that the aromatic groups of the polymer are  $\pi$ -stacked.

Chiral conformational features of **1**, **2**, **3**, and the polymer were next investigated. Figure 4 shows the UV-CD spectra of **1** (A), **2** (B), **3** (C), the polymer (D) along with those of BINOL (E). In the CD spectrum of **1**, an intense, negative Cotton splitting centered at 228 nm was observed in addition to less intense, two positive Cotton bands at 244 and 291 nm and a negative band at 264 nm. The former splitting is very similar to



**Figure 1.** SEC curves for the products obtained by reactions at different monomer concentrations at 23 °C for 24 h (A), at [BINOL] = [PDI] = 0.154 M at different temperatures for 24 h (B), and at [BINOL] = [PDI] = 0.154 M at 23 °C for different reaction durations (C). The reactions in A and B were quenched by exposure to air, and those in C by the addition of MeOH.



**Figure 2.** Crystal structure of cyclic dimer (1); top and side views where gray, blue, red, and white objects correspond to C, N, O, and H atoms.

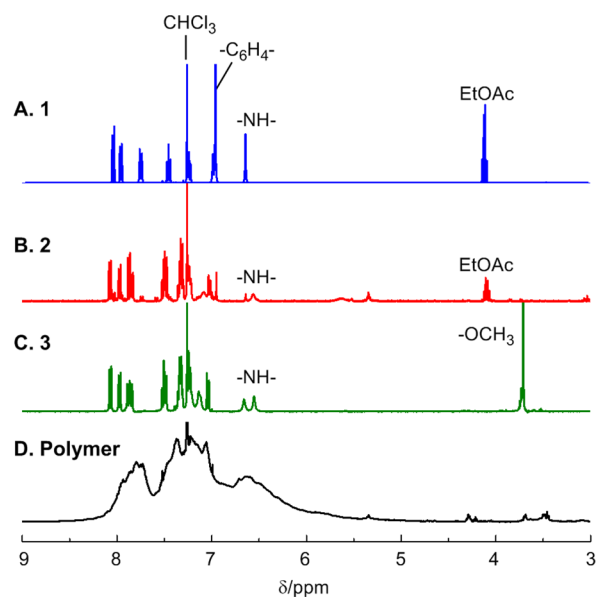


**Figure 3.** <sup>1</sup>H NMR spectra of 1 (A), 2 (B), 3 (C), and poly(BINOL-PDI) (D); 400 MHz, CDCl<sub>3</sub>, 23 °C, Me<sub>4</sub>Si.

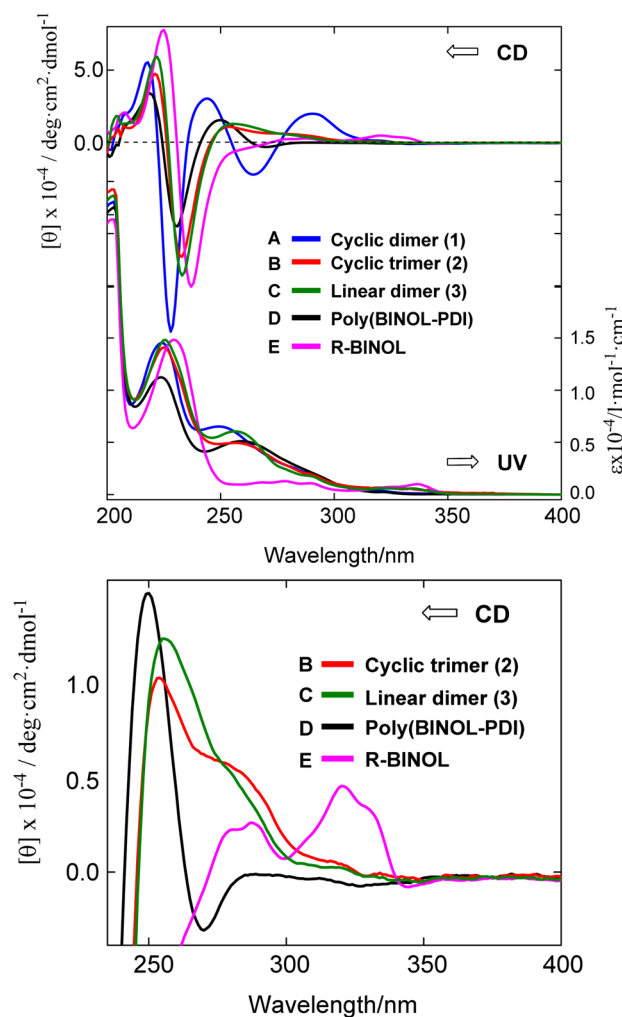


**Figure 4.** CD-UV spectra of **1** (A), **2** (B), **3** (C), poly(BINOL-PDI) (D), and R-BINOL (E) (top) and expanded CD spectra of **2** (B), **3** (C), poly(BINOL-PDI) (D), and R-BINOL (E) (bottom; THF, 23 °C, [BINOL] or [3] or [residue] =  $1.0 \times 10^{-4}$  M, cell path 1 mm). Residues for **1** and **2** means a unit consisting of a BINOL and a -CO-NH-C<sub>6</sub>H<sub>4</sub>-NH-CO- moieties.

that in the spectrum of BINOL (Figure 4E) in pattern but is blue-shifted compared with BINOL by 9 nm, while the latter three bands are missing in the BINOL spectrum. These results suggest that the former CD bands mainly reflect chirality of the BINOL moiety in **1** and the latter bands arise mainly from chirality of the two -CO-NH-C<sub>6</sub>H<sub>4</sub>-NH-CO- moieties, which is supported by the fact that dimethyl 1,4-phenylenedicarbamate, prepared separately as a reference compound, indicated a UV band in the range of 225–275 nm peaked at 255 nm (SI, Figure S12). The -CO-NH-C<sub>6</sub>H<sub>4</sub>-NH-CO- moieties may contribute to the CD spectra due to axial chirality around the single bonds connecting CO, NH, and benzene fragments and also chiral alignment between the two moieties.

The fact that the BINOL-based splitting is blue-shifted for **1** suggests that the dihedral angle of the BINOL moieties of **1** is greater than that of BINOL. This is supported by the fact that the averaged dihedral angle of **1** in crystal and the angle of BINOL according to molecular mechanics calculations (COMPASS force field) were  $-92.2^\circ$  and  $-64.0^\circ$ , respectively.

The CD spectra of **2** and **3** appear similar to each other, with the BINOL-based splitting centered at around 233 nm. In the

longer-wavelength range, the spectra of **2** and **3** had positive peaks at around 255 nm and monotonously decreased in intensity to zero as the wavelength increased to 350 nm. Such spectral characters are not observed in the R-BINOL spectrum, indicating that CD spectra in this range mainly reflect chirality of the -CO-NH-C<sub>6</sub>H<sub>4</sub>-NH-CO- moieties. Further, the spectral patterns of **2** and **3** were largely different from that of **1** in the fact that they lack the negative band at 264 nm and the positive band at 291 nm. In order to assess this point, the structures of **2** and **3** were examined by molecular dynamics simulations (COMPASS force field; SI, Figures S22 and S23) and compared with the structure of **1** in crystal. The most noticeable difference in conformation of the three compounds is that the two -C<sub>6</sub>H<sub>4</sub>- groups in **2** and two of the three -C<sub>6</sub>H<sub>4</sub>- groups in **3** are rather parallel to each other, while they are rather perpendicularly aligned in **1**. The intense CD bands at 264 and 291 nm may arise from the perpendicular alignment of the two -C<sub>6</sub>H<sub>4</sub>- groups.

In the CD spectrum of the polymer, the BINOL-based splitting is centered at 231 nm, and the longer-wavelength bands appear more similar to those of **1** in the range of 245–280 nm, rather than those of **2** and **3**. The spectrum of the polymer has a positive peak at 250 nm and a trough with a minimum at 271 nm, although the intense positive peak of **1** at 291 nm was not seen for the polymer. These results suggest that there are similarities between conformations of the polymer and **1**. The -CO-NH-C<sub>6</sub>H<sub>4</sub>-NH-CO- moieties in the polymer are in chiral environment though their alignment and internal rotation may not be as strongly restricted as those in **1**.

The UV spectra of **1**, **2**, **3**, the polymer, and BINOL provide important information on conformations of these species. The BINOL-based bands of the polymer had lower intensity (hypochromicity) than those of **1**, **2**, **3**, and BINOL, where  $\epsilon$  at 224 nm of the polymer was  $11280 \text{ L mol}^{-1} \text{ cm}^{-1}$ , while  $\epsilon$  at 229 nm of **1** was  $145400 \text{ L mol}^{-1} \text{ cm}^{-1}$ ,  $\epsilon$  at 225 nm of **2** was  $140940 \text{ L mol}^{-1} \text{ cm}^{-1}$ ,  $\epsilon$  at 225 nm of **3** was  $146010 \text{ L mol}^{-1} \text{ cm}^{-1}$ , and  $\epsilon$  at 229 nm of BINOL was  $148040 \text{ L mol}^{-1} \text{ cm}^{-1}$ . Hypochromic effects of the polymer were also observed at around 260 nm with respect to **1** and **3**, though the extent was smaller at 224 nm. These observations suggest that aromatic groups in the polymer are  $\pi$ -stacked. Hypochromicity is well-known for stacked base pairs of DNAs.<sup>9</sup>  $\pi$ -Stacking is further supported by the NMR spectrum, as discussed earlier. Relations between a  $\pi$ -stacked conformation with hypochromic effects in UV spectra and upfield shifts in NMR spectra have been established for vinyl polymer systems.<sup>10</sup>

Considering the findings discussed so far and viewing **1** and **3** as embryonic structures of the linear polymer, we propose a  $\pi$ -stacked, 2/1-helical conformation in which the BINOL units are “turn” moieties changing the direction of the main chain (Figure 5). The structure in Figure 5 was created on the basis of the structure of **1** and was optimized by molecular dynamics simulations at 298 K for 21 ns followed by molecular mechanics minimization; it accounts for the stacking and chirality of the -CO-NH-C<sub>6</sub>H<sub>4</sub>-NH-CO- moieties. The alignments of -C<sub>6</sub>H<sub>4</sub>- groups in the main chain are not completely parallel, which may explain the CD pattern of the polymer in the range of 245–280 nm.

The average spacing between neighboring BINOL units and that between neighboring phenylene units, as measured as C1-to-C8 (naphthyl moiety) distance and C1-to-C4 (phenylene moiety) distance were about 7.6 and 4.5 Å, respectively, in the model shown in Figure 5 (SI, Figure S25). Although the former



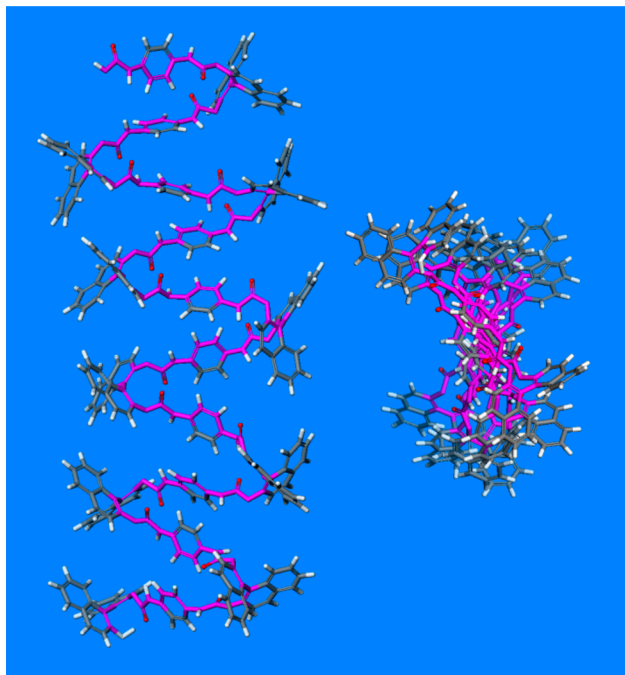


**Figure 5.** A 10-mer linear polymer model having a  $\pi$ -stacked 2/1-helical conformation obtained through molecular dynamics simulations at 298 K for 21 ns and molecular mechanics optimization: side (left) and top (right) views.

spacing is greater than typical distances of  $\pi$ -stacking, closer alignments of BINOL units can occur in conformational dynamics of the rather restricted conformation and may contribute to the hypochromicity in the averaged absorbance spectra in Figure 4. The latter spacing may be reasonable for  $\pi$ -stacking because interchain  $\pi$ -stacking distance of 4.4 Å has been reported for a conjugated polymer.<sup>11</sup>

The proposed conformation seemed to be stable in the range of temperature of  $-5$  to  $60$  °C. No clear changes in shape and intensity in CD and  $^1\text{H}$  NMR spectra were observed in this range of temperature (SI, Figures S3 and S10). The stability was also supported by molecular dynamics simulations at 398 K for 21 ns where the 2/1-helical conformation was maintained. Although properties of polyurethanes are often based on their hydrogen bond formation between chains,<sup>1</sup> hydrogen bonding may not have a crucial contribution in forming and maintaining the proposed conformation on the basis of the conformational stability in the wide range of temperature.

In summary, we found that cyclic oligomers and linear polymer are formed in the reaction between BINOL and PDI. Selectivity of linear chain or cyclic compounds can be tuned by changing reaction conditions. The linear polymer appears to possess a novel,  $\pi$ -stacked 2/1-helical conformation. 2/1-Helical conformation has been known only for limited types of polymers, including syndiotactic polystyrene, poly(*p*-methylstyrene), and some polydienes in the solid state,<sup>8</sup> and is unprecedented for other polymers. Further, because  $\pi$ -stacked conformation is known to facilitate charge mobility and photoelectronic properties,<sup>10,12–15</sup> the polymer prepared in this work may find novel applications for which polyurethanes have never been used. Further, the design of the polymer chain based on a rigid diol and diisocyanate may be expanded to a wider variety of polyurethanes having a  $\pi$ -stacked, helical conformation.

## ■ ASSOCIATED CONTENT

### 📄 Supporting Information

Experimental details,  $^1\text{H}$  NMR and IR spectra, mass profiles, and molecular structures. The Supporting Information is available free of charge on the ACS Publications website at DOI: 10.1021/acsmacrolett.5b00477.

(PDF)

## ■ AUTHOR INFORMATION

### Corresponding Author

\*E-mail: tamaki.nakano@cat.hokudai.ac.jp.

### Notes

The authors declare no competing financial interest.

## ■ ACKNOWLEDGMENTS

We thank Dr. K. Yoza (Bruker AXS) for technical advice on crystallographic analysis. T.N. acknowledges The Mitsubishi Foundation for financial support.

## ■ REFERENCES

- (1) For selected reviews on polyurethane synthesis and characteristics: (a) Delebecq, E.; Pascault, J.-P.; Boutevin, B. *Chem. Rev.* **2013**, *113*, 80–118. (b) Krol, P. *Prog. Mater. Sci.* **2007**, *52*, 915. (c) Wicks, D. A.; Wicks, Z. W. *Prog. Org. Coat.* **1999**, *36*, 148. (d) Wicks, D. A.; Wicks, Z. W. *Prog. Org. Coat.* **2001**, *41*, 1. (e) Wicks, D. A.; Wicks, Z. W. *Prog. Org. Coat.* **2001**, *43*, 131. (f) Caraculacu, A. A.; Coseri, S. *Prog. Polym. Sci.* **2001**, *26*, 799.
- (2) (a) Chen, Y.; Lin, J.-J. *J. Polym. Sci., Part A: Polym. Chem.* **1992**, *30*, 2699–2707. (b) Kobayashi, T.; Kakimoto, M.-a.; Imai, Y. *Polym. J.* **1993**, *25*, 969–975.
- (3) (a) Okamoto, Y.; Nakano, T. *Chem. Rev.* **1994**, *94*, 349–372. (b) Nakano, T.; Okamoto, Y. *Chem. Rev.* **2001**, *101*, 4013–4038. (c) Yashima, E.; Maeda, K.; Iida, H.; Furusho, Y.; Nagai, K. *Chem. Rev.* **2009**, *109*, 6102–6211. (d) Yashima, E.; Maeda, K.; Okamoto, Y. *Nature* **1999**, *399*, 449–451. (e) Shimomura, K.; Ikai, T.; Kanoh, S.; Yashima, E.; Maeda, K. *Nat. Chem.* **2014**, *6*, 429–434. (f) Nakano, T. *Chem. Rec.* **2014**, *14*, 369–385. (g) Nakano, T. *J. Chromatogr. A* **2001**, *906*, 205–225. (h) Green, M. M.; Park, J.-W.; Sato, T.; Teramoto, A.; Lifson, S.; Selinger, R. L. B.; Selinger, J. V. *Angew. Chem., Int. Ed.* **1999**, *38*, 3138–3154. (i) Deming, T. J.; Novak, B. M. *J. Am. Chem. Soc.* **1992**, *114*, 7926–7927. (j) Yu, Z.; Wan, X.; Zhang, H.; Chen, X.; Zhou, Q. *Chem. Commun.* **2003**, *48*, 974. (k) Wang, Y.; Sakamoto, T.; Koyama, Y.; Takanashi, Y.; Kumaki, J.; Cui, J.; Wan, X.; Nakano, T. *Polym. Chem.* **2014**, *5*, 718–721.
- (4) (a) Pu, L. *Chem. Rev.* **1998**, *98*, 2405–2494. (b) Pu, L. *Chem. - Eur. J.* **1999**, *5*, 2227–2232. (c) Hu, Q. S.; Vitharana, D.; Liu, G.-Y.; Jain, V.; Wagaman, M.-W.; Zhang, L.; Lee, T.-R.; Pu, L. *Macromolecules* **1996**, *29*, 1082–1084. (d) Hu, Q.-S.; Zheng, X.-F.; Pu, L. *J. Org. Chem.* **1996**, *61*, 5200–5201. (e) Ma, L.; Hu, Q.-S.; Vitharana, D.; Wu, C.; Kwan, C.-M.-S.; Pu, L. *Macromolecules* **1997**, *30*, 204–218. (f) Wyatt, S.; Hu, Q.-S.; Yan, X.-L.; Bare, W. D.; Pu, L. *Macromolecules* **2001**, *34*, 7983–7988. (g) Takata, T.; Furusho, Y.; Murakawa, K.-i.; Endo, T.; Matsuoka, H.; Hirasa, T.; Matsuo, J.; Sisido, M. *J. Am. Chem. Soc.* **1998**, *120*, 4530–4531.
- (5) Chen, J.; Zhang, J.; Huang, S.-H.; Wu, Y.-X.; Bai, Z.-W. *Fenxi Kexue Xuebao* **2009**, *25* (2), 161–165.
- (6) (a) Mengerink, Y.; Peters, R.; Kerkhoff, M.; Hellenbrand, J.; Omlou, H.; Andrien, J.; Vestjens, M.; van der Wal, S. *J. Chromatogr., A* **2000**, *876*, 37–50. (b) Mengerink, Y.; Peters, R.; deKoster, C. G.; van der Wal, S.; Claessens, H. A.; Cramers, C. A. *J. Chromatogr., A* **2001**, *914*, 131–145. (c) Mengerink, Y.; Peters, R.; van der Wal, S.; Claessens, H. A.; Cramers, C. A. *J. Chromatogr., A* **2002**, *949*, 307–326.
- (7) Ruddick, C. L.; Hodge, P.; Cook, A.; McRiner, A. J. *J. Chem. Soc., Perkin Trans. 1* **2002**, 629–637.

(8) (a) Chatani, Y.; Inagaki, Y.; Shimane, Y.; Ijitsu, T.; Yukimori, H.; Shikuma, H. *Polymer* **1993**, *34*, 1620–1624. (b) Chatani, Y.; Inagaki, T.; Shimane, Y.; Shikuma, H. *Polymer* **1993**, *34*, 4841–4845. (c) De Rosa, C.; Rizzo, P.; Ruiz de Ballesteros, O.; Petraccone, B.; Guerra, G. *Polymer* **1999**, *40*, 2103–2110. (d) Petraccone, V.; La Camera, D.; Pirozzi, B.; Rizzo, P.; De Rosa, C. *Macromolecules* **1998**, *31*, 5830–5836. (e) Pirozzi, B.; Napolitano, R.; Giusto, G.; Ricci, G. *Macromol. Chem. Phys.* **2008**, *209*, 1012–1020.

(9) (a) Tinoco, I. *J. Am. Chem. Soc.* **1960**, *82*, 4785. (b) Rhodes, W. J. *Am. Chem. Soc.* **1961**, *83*, 3609. (c) Watson, J. D.; Crick, F. H. C. *Nature* **1953**, *171*, 737–738.

(10) (a) Nakano, T.; Takewaki, K.; Yade, T.; Okamoto, Y. *J. Am. Chem. Soc.* **2001**, *123*, 9182–9183. (b) Nakano, T.; Yade, T. *J. Am. Chem. Soc.* **2003**, *125*, 15474–15484. (c) Nakano, T.; Yade, T.; Fukuda, Y.; Yamaguchi, T.; Okumura, S. *Macromolecules* **2005**, *38*, 8140–8148. (d) Nakano, T. *Polym. J.* **2010**, *42*, 103–123. (e) Nakano, T.; Yade, T.; Yokoyama, M.; Nagayama, N. *Chem. Lett.* **2004**, *33*, 296–297. (f) Nakano, T.; Nakagawa, O.; Tsuji, M.; Tanikawa, M.; Yade, T.; Okamoto, Y. *Chem. Commun.* **2004**, *2*, 144–145. (g) Nakano, T.; Tanikawa, M.; Nakagawa, O.; Yade, T.; Sakamoto, T. *J. Polym. Sci., Part A: Polym. Chem.* **2009**, *47*, 239–246.

(11) Meng, B.; Song, H.; Chen, X.; Xie, X.; Liu, J.; Wang, L. *Macromolecules* **2015**, *48*, 4357–4363.

(12) (a) Morisaki, Y.; Chujo, Y. *Angew. Chem., Int. Ed.* **2006**, *45*, 6430–6437. (b) Morisaki, Y.; Chujo, Y. *Prog. Polym. Sci.* **2008**, *33*, 346–364.

(13) (a) Knoblock, K. M.; Silvestri, C. J.; Collard, D. M. *J. Am. Chem. Soc.* **2006**, *128*, 13680–13681. (b) Jagtap, S.; Mukhopadhyay, S.; Coropceanu, V.; Brizius, G. L.; Brédas, J.-L.; Collard, D. M. *J. Am. Chem. Soc.* **2012**, *134*, 7176–7185.

(14) (a) Cappelli, A.; Mohr, G. P.; Anzini, M.; Vomero, S.; Donati, A.; Casolaro, M.; Mendichi, R.; Giorgi, G.; Makovec, F. *J. Org. Chem.* **2003**, *68*, 9473–9476. (b) Cappelli, A.; Galeazzi, S.; Giuliani, G.; Anzini, M.; Grassi, M.; Lapasin, R.; Grassi, G.; Farra, R.; Dapas, B.; Aggravi, M.; Donati, A.; Zetta, L.; Boccia, A. C.; Bertini, F.; Samperi, F.; Vomero, S. *Macromolecules* **2009**, *42*, 2368–2378.

(15) Sugino, H.; Koyama, Y.; Nakano, T. *RSC Adv.* **2015**, *5*, 21310–21315.